Research Square

Preprints are preliminary reports that have not undergone peer review.
They should not be considered conclusive, used to inform clinical practice,
or referenced by the media as validated information.

Reversing Degradation: Recovery of Ion-Induced Performance Losses in Perovskite Solar Cells

Felix Lang

lang1@uni-potsdam.de

University of Potsdam https://orcid.org/0000-0001-9711-380X

Paria Forozi Sowmeeh

Institute of Physics and Astronomy University of Potsdam

Jarla Thiesbrummel

University of Potsdam

Andres Felipe Castro Mendez

University of Potsdam

Sahil Shah

University of Queensland

Biruk Alebachew Seid

Institute of Physics and Astronomy University of Potsdam

Francisco Peña-Camargo

Helmholtz-Zentrum Berlin für Materialien und Energie

Thomas Hultzsch

University of Potsdam

Jan Hagenberg

University of Potsdam

Martin Stolterfoht

CUHK

Article

Keywords:

Posted Date: May 18th, 2026

DOI: https://doi.org/10.21203/rs.3.rs-9643570/v1

License: This work is licensed under a Creative Commons Attribution 4.0 International License.
Read Full License

Additional Declarations: There is **NO** Competing Interest.

Reversing Degradation: Recovery of Ion-Induced Performance Losses in Perovskite Solar Cells

Paria Forozi Sowmeeh [a], *Jarla Thiesbrummel* [a,b]*, *Andres Felipe Castro Mendez* [a], *Sahil Shah* [c], *Biruk Alebachew Seid* [a], *Francisco Peña-Camargo* [d], *Thomas Hultzsch* [a], *Jan Hagenberg* [a], *Martin Stolterfoht* [e], *Felix Lang* [a] *

[a] Institute of Physics and Astronomy, University of Potsdam, Potsdam-Golm, Germany

[b] Humboldt University Berlin, Germany

[c] University of Queensland, Australia

[d] Helmholtz-Zentrum Berlin für Materialien und Energie, Berlin, Germany

[e] Electronic Engineering Department, The Chinese University of Hong Kong, Hong Kong SAR, China

*Corresponding Authors: felix.lang1@uni-potsdam.de, jarla.thiesbrummel.2@uni-potsdam.de

Abstract

Although perovskite solar cells (PSCs) are widely recognized for their partial self-healing behaviour, the fundamental mechanisms linking degradation and recovery remain poorly understood, particularly the role of mobile ions. By directly comparing a stable and a poorly stable system, we demonstrate in this work that characterization at the fresh stage alone is inadequate to predict long-term stability or ionic behaviour. Instead, light/dark cycling emerges as a reliable indicator, unveiling the cumulative nature of ion-driven degradation, which ultimately dictates the extent and reversibility of performance losses. Intriguingly, devices that appear to exhibit minimal ionic effects in their fresh state can evolve into highly unstable systems under operation, while others with stronger initial ionic signatures may demonstrate greater operational stability. Furthermore, we identify temperature and dark resting time as important control parameters for regulating ion migration and recovery. Together, these findings highlight test protocols based on light/dark cycling as a transformative approach for understanding and controlling degradation, offering new pathways toward extending the lifetime of PSCs.

Introduction

Nature is dynamic and intrinsically capable of repairing itself. From the gradual healing of wounds in the human body at the micro scale to ongoing cellular repair in living organisms at the macroscale, self-healing is embedded as a fundamental strategy for survival. Yet perovskite solar cells (PSCs) are developed without incorporating this principle of resilience, and despite achieving remarkable power conversion efficiencies (PCEs), they remain poorly stable largely due to ion migration; they degrade under illumination, which is the very stimulus essential for their operation.[1–3] Understanding and harnessing self-healing mechanisms within perovskite materials might transform intrinsic instability from a critical limitation into a more controllable and potentially reversible process.

The ABX_3 components of perovskite are bound through relatively weak ionic, hydrogen, and Van der Waals interactions,[4–6] thereby classifying metal halide perovskites as soft ionic semiconductors as opposed to covalent bonds in traditional solar cell materials like silicon. The soft lattice of perovskites, combined with low defect formation energies and low ion migration barriers[7,8] allows for local lattice relaxation, dynamic defect generation, and annihilation. This facilitates efficient defect diffusion-recombination processes, conferring an inherent self-healing characteristic.

The mixed ionic-electronic conductivity of metal halide perovskites arises from ionic transport under external stimuli such as applied electric field, illumination, or thermal activation.[9–13] Ion migration in these materials is predominantly mediated by lattice defects, with halide-related defects, particularly iodide vacancies, identified as the most mobile species due to their comparatively low activation energies of migration (E_a).[14–16] An immediate consequence of charged migrating species is field screening, [17–19] deteriorating device performance. Beyond these electrostatic effects, ion migration may also facilitate the formation of deep defects, [20] trigger chemical and structural degradation within the bulk and at interfaces, and in severe cases, shunting of the PSC.

In some cases, band bending resulting from ion redistribution can suppress interfacial recombination, leading to an improvement in open-circuit voltage (V_{OC}) and giving rise to the light-soaking effect. [21] Additionally, the accumulation of mobile ions at the perovskite interfaces and the resulting electrostatic field screening can also lead to noticeable current losses[22] as well as a reduction in fill factor (FF)[19]. Furthermore, mobile ions may contribute to

a mismatch between the V_{OC} and the quasi-Fermi level splitting ($QFLS$),[21] resulting in additional V_{OC} losses. As one of the effects of continuous aging, enhanced field screening can further accelerate the generation of mobile ions, leading to the formation of deep defects[23], halide segregation[24], and ion–metal interfacial reactions. [25–27]

However, owing to the intrinsically soft ionic lattice of the metal halide perovskites, not all of these ion-induced effects are necessarily permanent. At early stages, ion-induced degradation can be reversible upon removal of the external stressor, as mobile ions redistribute and previously generated defects are annihilated during subsequent relaxation in the dark. This dynamic defect re-equilibration enables partial self-healing of the device performance. Consequently, rather than allowing degradation mechanisms to accumulate during prolonged operation, implementing periodic "dark resting" intervals can significantly enhance long-term stability and improve overall device durability. [28,29]

Under illumination, photogenerated carriers perturb the defect equilibria by modifying the quasi-Fermi level positions, thereby enabling the formation energies of charged ionic defects to be reached and driving their migration. In particular, photogenerated holes can participate in iodide defect chemistry and drive the formation of an iodide Frenkel pair according to [14,30]

$$I_I^x + h \rightleftharpoons I_i^x + V_I \qquad \textbf{Equation (1)}$$

Where I_I^x denotes a lattice iodide, I_i^x an interstitial iodide, and V_I an iodide vacancy. This results in the creation of mobile interstitial halide and halide vacancies. The interstitial iodide can subsequently undergo bond formation to produce molecular iodine via

$$2I_i^x \rightleftharpoons I_2 \qquad \textbf{Equation (2)}$$

enabling iodine evolution at the interfaces and bulk. Upon halting illumination, the electronic carrier population decreases, and the equilibrium shifts back toward the left-hand side of the reaction, promoting recombination of interstitial iodide and vacancies and dissociation of I_2, provided it is still present in the perovskite. This reversible, light-driven defect formation and subsequent annihilation in dark conditions highlights the dynamic halide chemistry of metal halide perovskites and provides the mechanistic basics for their self-healing under operational conditions. [11,30]

In a study by Domanski et al.,[31] it was proposed that cation vacancies migrate over long time scales (>10^3 s) and accumulate at the electron-transport contact, leading to reversible performance losses that are fully recoverable when the device is left in the dark. Consistent

with this, Jiang et al.[32] suggested that upon removal of illumination, the accumulated ions/vacancies diffuse back to their original bulk positions, thereby reducing interfacial charge build-up. However, they attributed the "fatigue behaviour" manifested as a progressive slowdown in recovery with increasing light/dark cycles to the repeated cyclic migration of these species under illumination. In this framework, the cumulative degradation is not directly caused by ionic motion itself, but rather by secondary, non-ionic processes that are progressively activated during cycling.

However, we recently found that ionic losses are only partially recoverable and may become locked-in after prolonged continuous illumination, e.g., maximum power point tracking over 1000 hours results in what can be described as "irreversible ionic losses". **Figure 1a** illustrates the evolution of the PCE of the perovskite solar cell undergoing 12 hours of continuous ageing, followed by a 12-hour dark resting. The incomplete restoration of PCE indicates the simultaneous presence of reversible and irreversible degradation mechanisms, progressively accumulating over successive cycles.

Recent outdoor studies on PSCs have indeed reported partial recovery in the dark, highlighting the practical relevance of ion migration under real operating conditions; however, these effects remain poorly understood, particularly in terms of their correlation with mobile ions, and are not consistently reproduced under controlled laboratory measurements. This underscores the need for testing protocols that better capture the dynamic nature of these materials, as well as for developing control strategies to actively manage recovery.

Furthermore, Khenkin et al.[33] aimed to predict the operational lifetime of the PSCs by analysing both indoor and outdoor behaviours. They demonstrate a remarkable dependence of the aging behaviour on the device architecture, as well as on the resulting transient behaviour and recovery dynamics. They further confirm that standard constant light exposure tests do not reliably predict real outdoor performance under light/dark cycling conditions. In contrast, cycling experiments show close agreement with the observed outdoor behaviour.

In another work,[33–36] they show that degradation is not monotonic, with PSCs exhibiting partial recovery during day-night cycles under outdoor conditions. This behaviour is explained by the simultaneous decrease in short circuit current (J_{sc}) and photoluminescent (PL) intensity under illumination, followed by their recovery in the dark, revealing reversible dynamics associated with light-induced metastable traps.

After more than a decade of stabilization efforts in PSC technology, it is therefore crucial to establish a deeper understanding of how degradation and recovery are governed by ionic processes, arguably the dominant factor in device instability, and to harness the intrinsically recoverable nature of perovskites to ultimately achieve stable, high-performance devices.[14,31]

In this study, we systematically investigate the contribution of mobile ions to the self-healing of PSCs under light/dark cycling conditions. **Figure 1a** illustrates the evolution and partial recovery of the PCE of the PSC under day/night cycling operation. Despite recovery during dark periods, a net PCE loss of ~5% accumulates over 156 hours, evidencing the presence of irreversible ionic losses. Here, we quantitatively assess the extent of performance recovery and the ionic contribution to this process under varying dark resting time and temperature. The observed recovery of degraded device performance is directly correlated with the re-migration or annihilation of mobile ions. Ion density and ionic losses increase during degradation under illumination, whereas both parameters significantly decrease after dark resting. We demonstrate that the reduction in ion density leads to substantial performance improvement following dark storage. Based on grazing-incidence XRD (GIXRD) measurements, recovery is attributed to the relaxation of tensile strain during dark resting, accompanied by the re-migration of mobile ions and partial annihilation of ionic defects.

Furthermore, we investigate the light/dark cycling behaviour of devices at different temperatures. Temperature-dependent, aging-recovery experiments reveal that PSCs degradation and subsequent recovery are strongly thermally activated. Devices exhibit limited degradation and full recovery at 0 °C, moderate reversible losses and good recovery at 25 °C, and significantly amplified degradation with little recovery at 55 °C. Complementary current density-voltage (*J-V)*, fast hysteresis (FH), and bias-assisted charge extraction (BACE) analyses confirm that elevated temperatures facilitate ion migration and generation of mobile ions, thereby increasing ionic losses and promoting reversible defect formation. These findings establish mobile ions as the dominant drivers of thermally activated instability and recovery in PSCs. Finally, we also look at the impact of different light/dark cycle durations, in an attempt to identify further pathways to control ionic performance loss and its recovery.

Result and discussion

We investigated two sets of perovskite solar cell compositions: $Cs_{0.05}(FA_{0.83}MA_{0.17})_{0.95}Pb(I_{0.83}Br_{0.17})_3$ with a bandgap of 1.63eV referred to shortly as "1.63 eV", and $Cs_{0.05}(FA_{0.95}MA_{0.05})_{0.95}Pb\,(I_{0.95}Br_{0.05}Cl)_3$ with slightly lower MA and Br content and a band gap of 1.58 eV referred to as "1.58 eV" throughout the paper. Full experimental procedures regarding device fabrication are detailed in the supporting information **(SI)**. The 1.63eV solar cell employs the architecture ITO/PTAA/PFN-Br/1.63 eV-perovskite/C60/BCP/Cu, while the 1.58eV solar cell consists of ITO/MeO-2PACz/1.58 eV-perovskite/C60/BCP/Cu. These configurations were intentionally selected as they represent two widely adopted and well-established benchmarks within the PSCs community. 1.58 eV SC is based on a composition that is widely used for enhanced operational stability [37] while the 1.63 eV has a composition with slightly higher Br content, featuring more ionic activities and halide segregation.[24,38] Notably, both compositions lie outside the range of strong halide segregation, i.e., beyond the compositional window where this effect is significant. In bulk cases, compositions with Br content < 20% are considered stable.[39,40] Accordingly, we note that the aim of this work is not to disentangle the specific impact of hole transport layer (HTL) or other interfacial layers; Instead, different hole transport layers were deliberately employed to reflect the standard stack configurations commonly used in literature.

To establish a benchmark of device performance, we recorded *J-V* characteristics **(Figure 1b).** The 1.58 eV device exhibits a PCE of 21.3% PCE on a fresh sample, whereas the 1.63eV sample exhibits a PCE of 19.5%. External quantum efficiency (*EQE*) measurements (**Figure 1c**) reveal the expected spectral cutoff shifts corresponding to the different band gaps.

GIXRD measurements performed at an incidence angle of $\omega = 3°$ were used to probe the crystalline structure of the perovskite in both 1.58 and 1.63 eV devices (**Figure 1d**). The GIXRD patterns confirm the formation of a predominantly cubic perovskite phase, with only small amounts of secondary phases such as PbI_2 (2θ =12.6), and different orientations as evidenced by variation in the (100)/(110) intensity ratio. The most significant structural difference between the two devices is a slightly smaller lattice parameter in the 1.63 eV device (**Figure 1d**). This lattice contraction is attributed to a higher bromide content, as the smaller ionic radius of Br^- compared to I^- leads to a reduction in the unit cell dimensions. [40]

To potentially differentiate the ionic species present in 1.58 and 1.63 samples, we performed temperature-dependent fast hysteresis (FH(T))[41,42] measurements. The FH method, introduced by Le Corre et al., quantifies ionic loss by recording *J-V* characteristics across a broad range of scan rates, where the steady-state (*SS*) PCE is defined at slow scan rates where reverse currents stabilise, reflecting equilibrium ionic redistribution. In contrast, the ion freeze PCE (*IF*) is determined at high scan rates, where the rapid change in applied electric field significantly exceeds the ionic diffusion timescale, effectively immobilizing mobile ions. Accordingly, the difference between the PCE_{SS} and PCE_{IF} represents the performance loss directly associated with ion migration (i.e., ionic loss). By determining the corresponding peak hysteresis scan rate and plotting these values as a function of 1/T(K) (**see Figure 1e and S1**), we extracted the activation energy (E_a) for the ion migration according to the Arrhenius law, $\nu_d = \nu_0 \exp\left(-\frac{E_a}{K_B T}\right)$. The 1.58eV device is characterized by a relatively high activation energy of E_a=0.89eV, whereas a substantial decrease to E_a=0.48eV is observed for the 1.63eV device, indicating facilitated ion migration in the latter. Furthermore, the peak hysteresis of the FH curve serves as an indicator of ionic mobility within the device. The mobile ions in the 1.63eV sample are characterized by significantly higher mobility (peak hysteresis scan rate $> 100\ \mathrm{Vs}^{-1}$) compared to $\approx 5\ \mathrm{Vs}^{-1}$ for the 1.58 eV sample, which is consistent with the lower migration barrier for the 1.63eV device. Therefore, the increased Br content in 1.63eV not only induces lattice contraction but also reduces the ion migration activation energy, thereby facilitating ionic mobility and migration.

FH measurement for both fresh devices reveals a small ionic loss (1.35%) for 1.63 eV compared to 2.18% for 1.58 eV (see **Figure 1f).** To evaluate the mobile ion density, BACE measurements were performed. The devices were initially held at open circuit voltage (V_{OC}) in the dark for a sufficiently long period (i.e., 100s) to allow mobile ions to redistribute uniformly within the perovskite layer. The bias was then abruptly switched to 0V, driving ions toward the perovskite/charge transport layer interfaces. Integrating the external current over 0V provides an estimate of mobile ion density. [19] **Figure 1g** suggests a smaller ion density present in the 1.63 eV sample. The lower ion density in the 1.63 eV device does not contradict the reduced activation energy for ion migration; rather, it indicates a system with fewer mobile ions that can migrate more readily due to the lower energy barrier. Taken together, the FH and BACE measurements of the fresh samples indicate a lower contribution of mobile ions in the 1.63eV;

however, this interpretation warrants further critical evaluations, as discussed in the following section.

Figure 1h represents the stable power output (SPO) tracking of both samples under continuous 1 sun conditions (solid lines). While the 1.58eV device exhibits a T80 of more than 200 hours with gradual performance improvement, the 1.63eV sample degrades to 80% of the initial PCE within the first 17 hours despite a lower ionic contribution for a fresh device. These markedly different stability trends suggest distinct underlying degradation mechanisms in two devices.

Next, to disentangle the reversible metastability and permanent degradation of the PSCs, device performance was investigated under multiple cycles of 1 hour at 1 sun illumination, followed by 1 hour of dark resting. **Figure 1h** represents the calculated PCEs derived from *J-V* measurement every 30 seconds for both devices under alternating light and dark cycles for 24 hours, with a cycle duration of 1 hour at 25°C. While the 1.63eV device undergoes a large PCE drop at each light cycle, followed by partial recovery during dark intervals, minimal degradation and full recovery are observed in the 1.58eV device.

The inset in **Figure 1h** represents the PCE of the devices under illumination, overlaid from the first to the last light cycle. While degradation and subsequent recovery are observable in the 1.63eV device, the 1.58eV device exhibits gradual performance improvement during successive cycles. This contrasting behavior highlights the different metastability characteristics of the two device types. Notably, degradation accelerates with each cycle in the 1.63eV device, and only a fraction of the performance loss is recoverable, while the remaining degradation becomes irreversible.

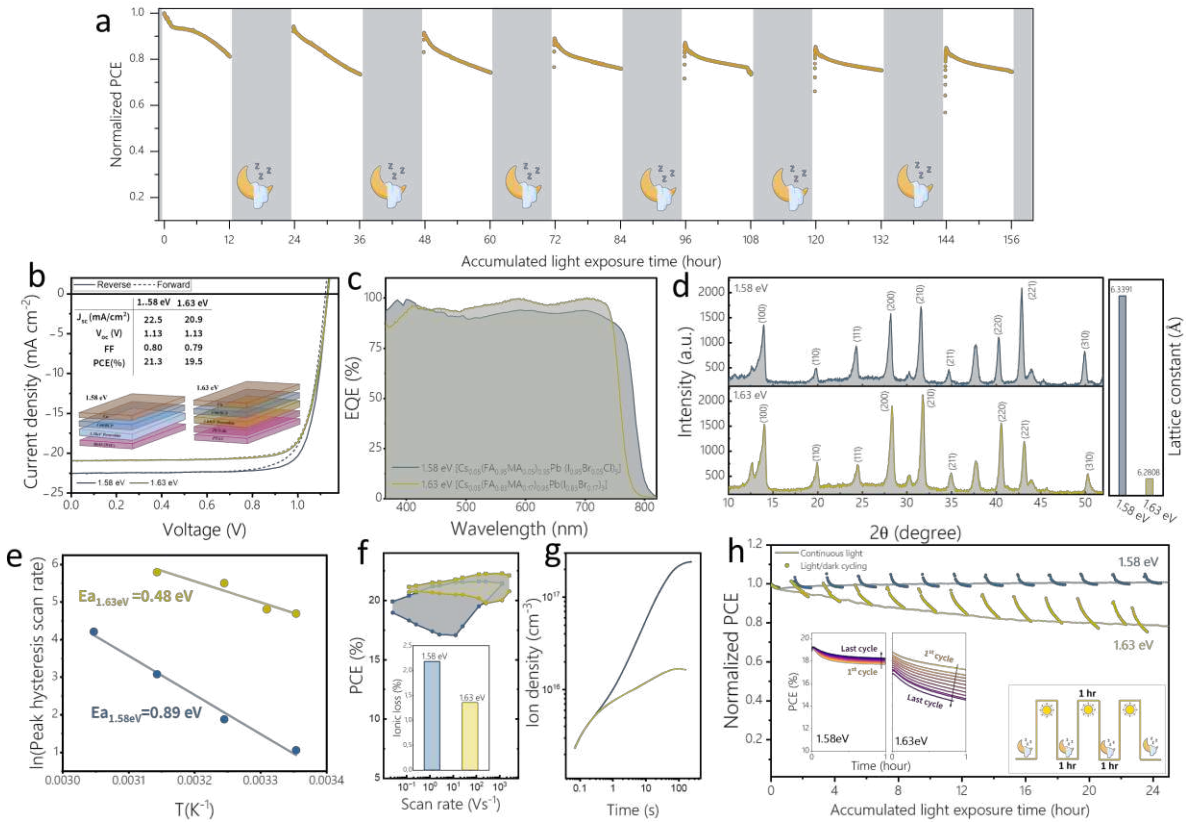


Figure 1: Different ionic activities in 1.58 and 1.63 eV PSCs. *a) Normalized PCE adopted from measuring J-Vs every 30 s under light/dark cycling with a period of 12 hours each, mimicking day-night cycles for the 1.63 eV sample. b) J-V measurement of fresh 1.58 and 1.63eV PSCs in reverse (solid lines) and forward (dashed lines). b) EQE measurement of the 1.58 and 1.63eV PSCs at the fresh stage. c)GIXRD of the 1.58 and 1.63eV PSCs at the fresh stage. d) lattice constant for 1.58 and 1.63eV PSCs. e) calculated activation energies from Arrhenius law and temperature-dependent fast hysteresis measurement. f) fast hysteresis measurement on 1.58eV and 1.63eV PSCs at the fresh stage. g) mobile ion density measured by the bias-assisted charge extraction method for both samples at the fresh stage. h) stabilized power point tracking as well as PCEs adopted from J-V measurement every 30s under light/dark cycling of the two samples under 1sun condition at 25°C.*

To elucidate the ion-induced recovery in more detail, we focus on the 1.63eV-type PSCs from here onwards, where the reversible degradation is more pronounced. **Figure 2a, b** represent the measured ionic PCEs and J_{sc} as a function of scan rates (refer to **Figure S2a, b** for *FF* and V_{oc}), adopted from FH measurement at 4 stages: i) fresh device, ii) after 1hour of 1 sun illumination, iii) after 1 hour of dark resting, and iv) after 48 hours of dark resting. Normalized photovoltaic parameters monitored during aging and recovery phases (see also **Figure S2c, d**) reveal that all parameters drop after light-induced aging. Within 1 hour of dark resting, *Voc* and J_{sc} partially recover, whereas the FF exhibits further deterioration. Upon extending the dark resting period to 48 hours, the FF also recovers, indicating a slower recovery process compared to V_{oc} and J_{sc} .

The reversible degradation of the 1.63eV PSC is linked to changes in the mobile ion density and ionic loss. The SS and IF normalized PCEs of the devices, subsequent to each stage extracted from FH measurements, are presented in **Figure 2c**. The ionic loss is plotted on the right-hand axis of the graph. Both SS and IF PCEs decrease after illumination, while the ionic loss increases up to 3 times its initial value; notably, the decrease in PCE_{ss} is more pronounced compared to PCE_{IF}. After 1 hour of dark resting, the ionic loss slightly decreases, indicating partial recovery of ion-induced losses. Finally, after 48 hours in the dark, ionic loss further decreases, and complete recovery is observed, accompanied by a continued reduction in ionic loss. Moreover, the losses under ion-freeze conditions recover, which is a clear sign that these losses, for the given aging time, are more determined by the specific (detrimental) ionic accumulation at the pre-bias before the start of the measurement rather than non-ionic losses in this particular sample.[43,44]

BACE measurements for 1.63eV device reveal that, while ion density increases to nearly 4 times the initial value (**Figure 2d and S2e**), leading to ~3% absolute ionic loss after 1 hour of illumination (**Figure 2c**), it reduces after 1hour of dark resting and almost returns to initial values after extending the dark resting time to 48 hours. The substantially larger reduction in PCE_{ss} compared to PCE_{IF} after illumination indicates that aging is predominantly governed by ion migration rather than irreversible chemical degradation.

Figure S3a shows an illumination-induced increase in mobile ion density in a 1.58 eV device after 1 hour at 1sun; however, after dark resting for 1 hour, the device exhibits a reduction in mobile ion density to a level even below that of the fresh device, consistent with ion immobilization or recombination of ions with vacancies in energetically favorable sites. In contrast, the 1.63eV (see **Figure 2d**) device maintains a relatively high ion density compared to the fresh sample, enabling partial recovery but ultimately promoting rapid performance decay under continuous operation. Moreover, FH (**Figure S3b**) demonstrates that while the 1.63eV device undergoes a pronounced ionic loss after illumination, accompanied by substantial ionic recovery during dark resting, the 1.58eV device shows a comparably very small level of ionic loss across all three stages.

The recovery proceeds through two distinct timescales, corresponding to fast (Rec_1) and slow (Rec_2) processes (refer to **Figure 2c**), which occur by resting the device in the dark for short (1 hour) and extended durations (up to 48 hours), respectively. Both ionic loss and ion density decrease during dark resting of the device up to a certain point (**Figure 2d**). However, beyond

this point, further dark storage does not lead to additional reduction in ionic loss, and the full recovery is observed. Consequently, the ionic loss returns to its initial value, and full recovery is achieved. On the other hand, a permanent loss in both SS and IF PCEs remains, indicating the presence of irreversible degradation components. Therefore, 1.63eV devices exhibit only partial recovery rather than full recovery after 1 hour of illumination. As a result, degradation accumulates over repeated light/dark cycles, which is a key factor contributing to their limited operational stability.

Light-induced holes generated during the aging process promote the breaking of Pb-I bonds, resulting in the formation of iodide interstitials (I_i) and iodide vacancies (V_I).[30] Upon removal of illumination and subsequent dark resting, a fraction of the generated iodide interstitials may remigrate and recombine with iodide vacancies, thereby reducing the ionic defect density. However, during 1 hour of dark resting, recombination remains incomplete, and the system does not return to its initial equilibrium. Instead, it relaxes toward a metastable state characterized by an elevated density of interstitial iodide and iodide vacancies, which accounts for the partial recovery alongside cumulative irreversible degradation observed during successive light/dark cycling (**Figure 1a**). Prolonged cycling further increases the defect density, with the degradation that adds up for every cycle and eventually disrupts the defect equilibrium, leading to permanent device degradation.

In-situ GIXRD diffractograms with a fixed incidence angle ω=1.0° were recorded to probe the structural evolution of the 1.63 eV perovskite layer during illumination and the subsequent dark recovery, thereby establishing a direct link between ionic defect dynamics and crystallographic changes. While the GIXRD does not change for 1hour of aging time (**Figure S4a, b**), we extended our measurement to 24 hours under illumination and 24 hours of recovery (**Figure 2e**). A rapid decay in peak intensity and peak broadening is observed under illumination (**Figure 2f and S4c**). Moreover, the perovskite peaks at $2\theta = 28.4°$ and $2\theta = 31.8°$ gradually shift to lower angles, indicating a widened lattice within the perovskite layer. On the other hand, the intensity of the peaks slightly increases in the first hours under dark conditions, but FWHM and position remain relatively constant. These results indicate that illumination triggers a rapid accumulation of compressive strain into the perovskite layer that

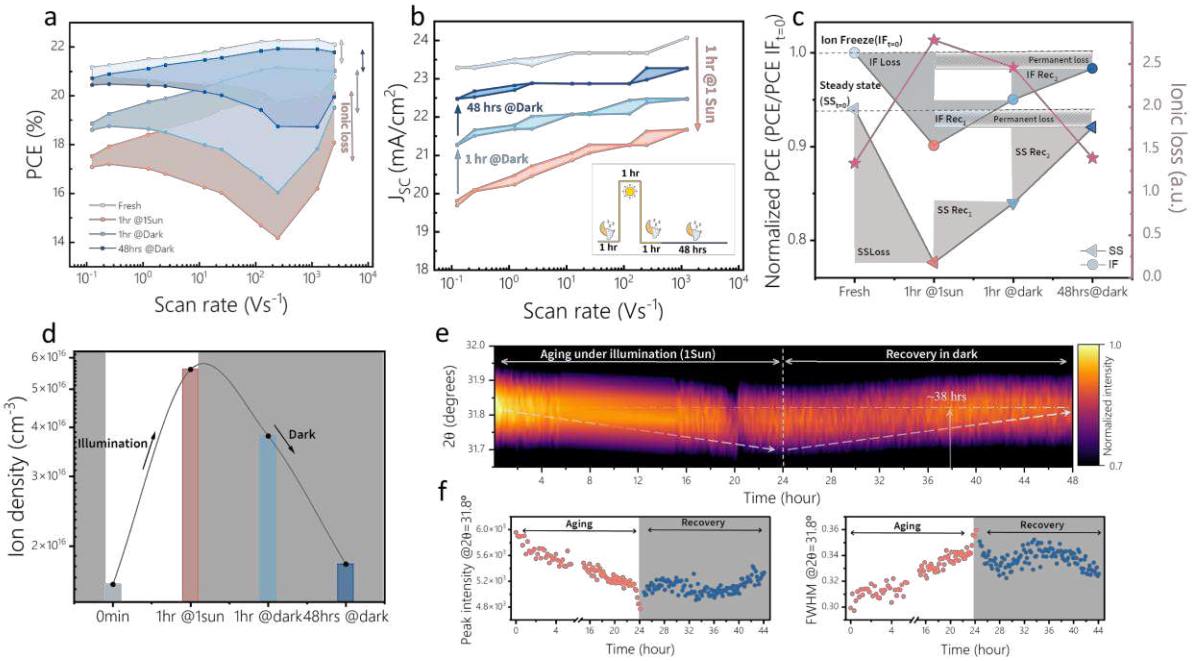


Figure 2: Mechanisms of recovery in PSCs. *a) FH measurement of the 1.63eV PSC at fresh, 1-hour aged, 1-hour recovery, and after 48 hours of recovery. b) J_{sc} as a function of scan rate at each stage of Fig. 2a, c) normalized PCEs and ionic loss (shown with stars) adapted from FH measurement. d) measured mobile ion density via BACE at different stages. e) In-situ GIXRD of the 1.63eV PSC under 24 hours of illumination and 24 hours of dark resting. f) $\theta = 31.8°$ peak intensity and FWHM of the sample, adapted from in-situ GIXRD with a fixed incidence angle $\omega = 1.0°$ during aging and recovery.*

correlates with the increase of mobile ion density in the device. This process is halted as soon as the light is turned off, as observed from the intensity, FWHM, and peak position during the recovery phase. However, the film needs more than 38 hours for the peak to return to its initial position. This long time to dissipate the compressive strain in the perovskite layer correlates with the time needed to largely decrease the mobile ion density in the device after light stress. Although the peak position recovers, the intensity and FWHM remain considerably lower than in the fresh device, indicating that the devices do not recover fully, and strain release might be accompanied by a decrease in the crystal size.

To understand how the optoelectronic properties of the perovskite change upon degradation and recovery, we also perform long-term PL measurements. **Figure 3a** represents the normalized PL peak intensity as a function of time for (i) an ITO/perovskite film measured under continuous 1 Sun illumination under a white light LED, (ii) the same film subjected to successive light/dark cycles with a dwell time of 1 hour, and (iii) a complete device stack measured under identical light/dark cycling conditions. In all cases, the PL spectra were acquired at 1-minute intervals.

For the ITO/perovskite films, the normalized PL intensity exhibits a monotonic decrease under both continuous illumination and cyclic light/dark operation. The degradation kinetics are comparable in both cases, and no discernible recovery occurs during the dark intervals. This behaviour indicates that light/dark cycling alone does not alleviate degradation in bare perovskite films. The absence of a built-in electric field during the dark period likely prevents the remigration of interstitial ionic defects toward adjacent vacancies, thereby inhibiting defect recombination and structural relaxation.

In contrast, the full device stack demonstrates pronounced PL recovery during light/dark cycling relative to the bare film despite going through a stronger loss under light. This distinct behaviour indicates that the recovery observed in perovskite solar cells is not an inherent property of the perovskite absorber alone, but rather emerges from the complete device architecture. Furthermore, the full stack displays a noticeable red shift in the PL emission after aging, indicating the formation of an iodide-rich domain, whereas the bare film shows no significant spectral shift (**Figure 3b and S5a-c**).

Spatially resolved PL mapping (**Figure 3c**) was employed to investigate the degradation and recovery dynamics in a full-stack device. Measurements were performed using a 50X objective, and the spectral evolution was quantified using the PL intensity ratio defined as I_{800nm}/I_{750nm}, which serves as a sensitive probe for band edge modifications and halide segregation. Two distinct regions were analysed: region A, located outside the intentionally illuminated area, and region B, positioned within the deliberately illuminated and degraded region.

Initially, PL was measured at low intensity to obtain the pristine state. In pristine state (**Figure S6**), the PL intensity under the low-intensity spot-illumination is spatially homogenous across the device, indicating a uniform bandgap and absence of sufficient halide segregation.

Subsequently, the device was exposed to high-intensity spot illumination for 60 minutes, after which PL was measured again (labelled “high intensity”). After 60 minutes of spot-illumination at high intensity (more than 1 sun), a pronounced increase in the PL intensity ratio is observed in region B while region A remains largely unaffected. The localized enhancement of the I_{800nm}/I_{750nm} ratio reflects a red shift of the PL emission in the degraded region and is consistent with photo-induced halide segregation and formation of iodide-rich domains. The spatial confinement of this effect confirms that the degradation process is locally driven by illumination.

Following the degradation step, the device was allowed to recover under low-intensity illumination. After 10 minutes of recovery, the PL ratio in region B began to decrease, accompanied by a reduction in spatial contrast between regions A and B, indicating the onset of recovery. After 60 minutes of resting under low intensity, the PL ratio in Region B approached that of Region A, and the spatial homogeneity of the PL maps is largely restored. However, the spectral PL characteristics of the recovered device did not fully return to those of the pristine sample, indicating only partial recovery. The partial reversibility is consistent with the trends observed in FH and BACE, suggesting that the recovery of the optoelectronic properties remains incomplete. Taken together, these findings suggest that photo-induced degradation in full perovskite devices is highly localized yet largely reversible.

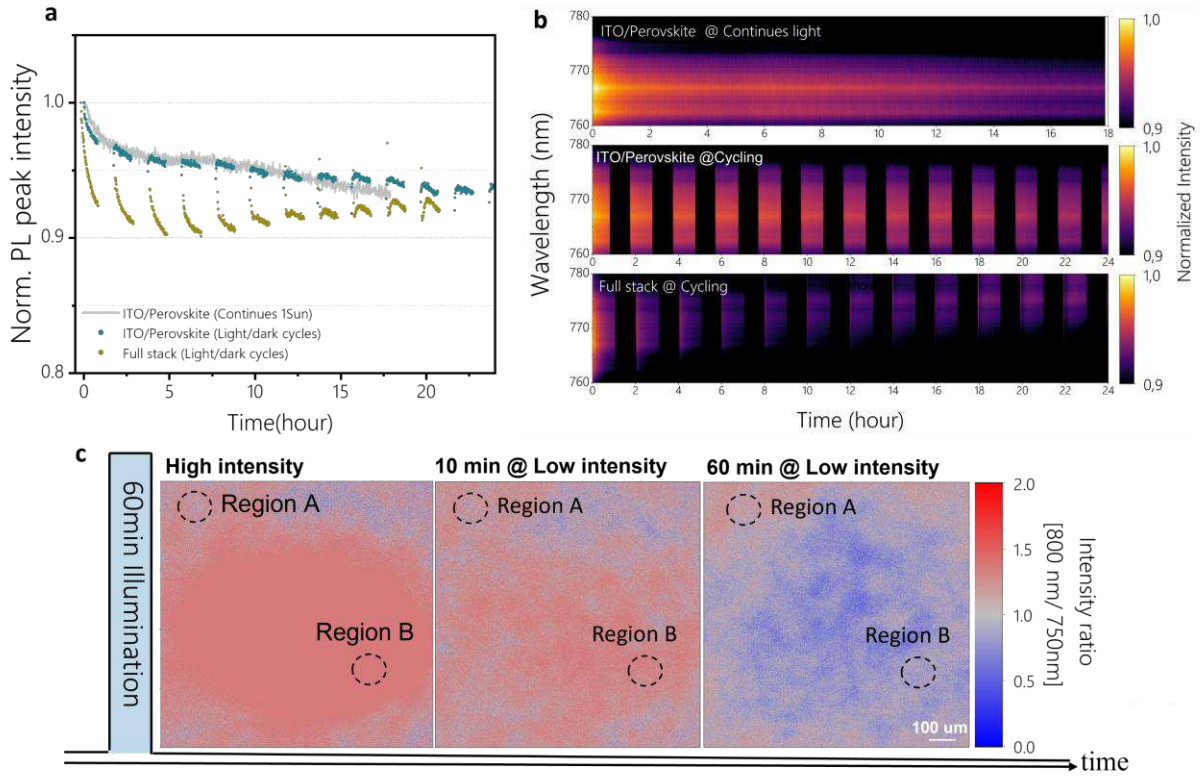


Figure 3 Recovery in PL *a) Normalized PL peak intensity of ITO/perovskite films under continuous and cycling light, as well as full stack under light/dark cycling b) wavelength vs. time for different samples mentioned in figure 3a. c) In-situ PL measurement during illumination and dark resting for a 1.63eV full stack.*

Finally, in an effort to identify potential control knobs for recovery beyond varying the duration of dark recovery periods, we investigated the impact of temperature and dark resting time on the recovery behavior of the PSCs. **Figure 4a** shows the normalized PCE extracted from *J–V* measurements acquired every 30 s during successive light/dark aging of full devices at 0, 25,

and 55°C while maintaining the devices at *J*sc condition in between measurements. Each cycle consists of a 1 h dwell period under 1 sun illumination, followed by a dark recovery period.

At 0 °C, the PCE remains comparatively stable, exhibiting limited degradation and full recovery of the performance between illumination and dark phases, indicating highly suppressed degradation pathways. In contrast, at 25 °C, clear aging behavior is observed during illumination, followed by partial recovery in the dark. This effect becomes significantly more pronounced at 55 °C, where both light and dark *J-V* show degradation. These trends are consistent with the temperature-dependent increase in both reversible losses (RL) obtained by and irreversible losses (IrrL) obtained by, as summarized in **Figure 4b**.

Figure 4c presents representative *J-V* characteristics prior to degradation at different temperatures. A marked reduction in J_{sc} under illumination is observed with increasing temperature, accompanied by pronounced hysteresis. The post-degradation *J-V* curves clearly show a strong decrease in *Jsc* (from 20 to 13 $\mathrm{mA/cm^2}$) at elevated temperatures.

Consistent with the *J-V* analysis, FH and BACE measurements taken on fresh and 24 h aged samples reveal pronounced ionic losses and a substantial increase in ion density at 55°C, indicating enhanced ion migration and accumulation over the course of the cycled aging experiment (**Figure 4d and e,** also see **Figure S7**). Notably, at room temperature, ionic losses remain dominant during the aging despite the cycling, highlighting their significant contribution to overall degradation under day-night cycling conditions. In contrast, at 0 °C, the ion density remains essentially unchanged even after 24 hours of cycling, and ionic losses are minimal. This can be attributed to the suppression of the generation of additional halide vacancies at low temperatures, resulting in reduced ionic polarization and diminished field screening.[45,46] Looking back to **Equation 1**, this observation suggests that ion-mediated degradation and recovery processes are strongly thermally activated not only in terms of migration but also in the creation of ion generation. In this context, the generation of vacancies is associated with an activation energy, and therefore, at lower temperatures, the reaction rate decreases, leading to a reduced density of mobile ions. As a result, both ion redistribution and the extent of ion-induced degradation are suppressed, confirming that thermally activated ionic processes are the dominant contributors to device instability at elevated temperatures.

To capture the rapid recovery of the device parameters, pseudo-light *J-V* curves were obtained by subtracting the dark *J-V* from the short-circuit current of the first illuminated *J-V* in the initial light cycle (I_{dark}-$I_{SC,\ light}$) (**Figure S8a, b**). This approach does not track *Jsc* recovery, and

therefore, any dark phase recovery of current cannot be captured in real time. Nevertheless, despite the dominance of current related losses, the method enables a clear observation of variations in *Voc* and *FF* during both the light and dark periods (see **Figure S9a, b**).

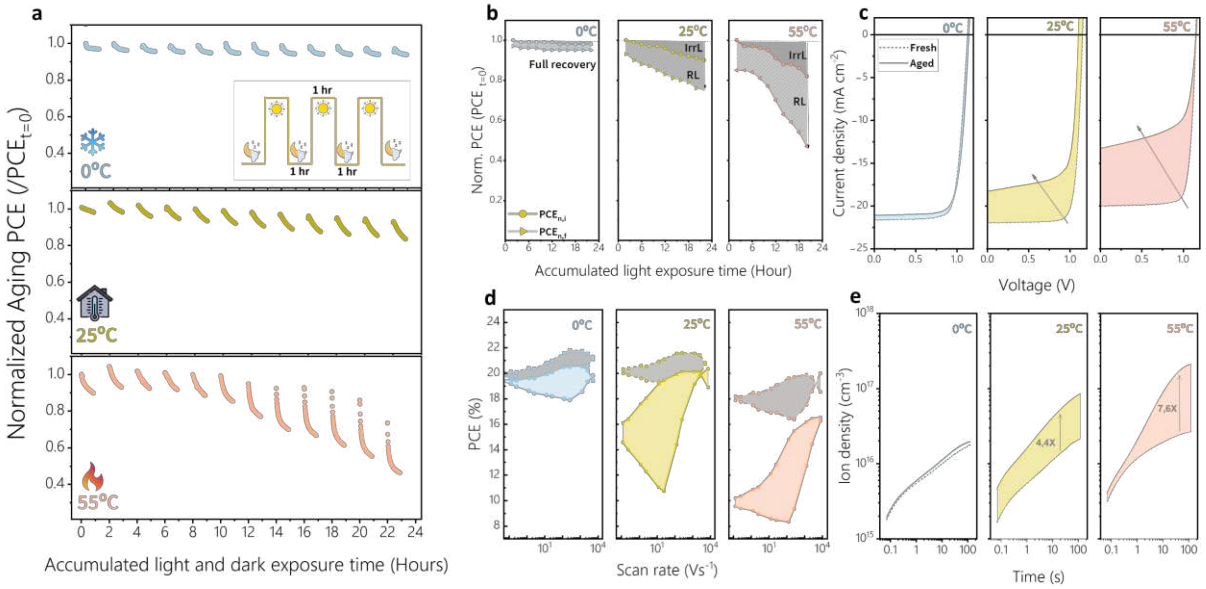


Figure 4: Temperature as a potential control knob for recovery. *a) normalized Aging 1.63eV PCEs at different temperatures, b) normalized PCEs explaining reversible and irreversible losses at different temperatures, c)J-Vs for a fresh and degraded sample at different temperatures. d) FH for a fresh and degraded device at different temperatures. e) ion density measurement for a fresh and degraded sample after 24 hours of light/dark cycling at different temperatures, c,d,e are measured at 25°C.*

Increasing the rest time of the PSC serves as an additional control parameter for enhancing recovery while minimizing degradation. As shown in **Figure 5a**, the 1.63eV device, when subjected to 2 hours of dark rest, maintains its efficiency with negligible J_{sc} degradation (**Figure S10a),** as well as minimal ionic loss (**Figure 5b**) and reduced ion density generation (**Figure 10b**). This result suggests that controlled light modulation, such as through the implementation of smart glass technologies[29], would help as an effective strategy for introducing recovery periods during PSC operation. By intermittently reducing illumination intensity, such systems may suppress ion generation and promote device recovery, thereby mitigating degradation pathways, ultimately extending device lifetime.

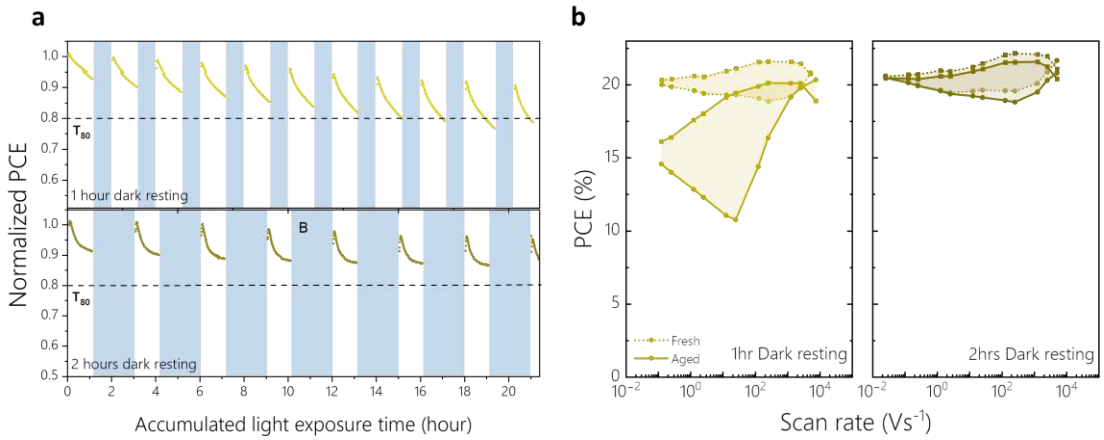


Figure 5. Dark period time as a potential control knob for recovery. *a) light/dark cycling with 1 hour of dark resting vs. 2 hours of dark resting, b) FH measurement at fresh and aged samples after 12 hours for different dark periods with reverse shown in (■) and forward in (●).*

Conclusion

In this work, we systematically investigated the reversible degradation and recovery in perovskite solar cells. Our study reveals that the reversible degradation in PSCs is governed by ion migration and defect relaxation, which dominate device metastability. Dynamic compositions exhibit high ion mobility, light-induced strain, and halide segregation, leading to pronounced performance loss that partially recovers during dark resting. In contrast, stable compositions exhibit a reduced ion mobility, minimizing both degradation and recovery dynamics, highlighting a clear mechanistic link between ionic activity, metastable lattice strain, and device performance. Temperature-dependent measurements confirm that ion-mediated processes are strongly thermally activated. These insights establish ion dynamics as a central control knob for PSCs' stability, providing pathways for designing more robust devices through management of defect kinetics and lattice relaxation.

The observed enhanced stability of the devices at 0 ºC suggests that temperature management could be a viable strategy to suppress ionic migration**.** Incorporating a passive cooling mechanism could maintain the perovskite layer at lower temperatures, minimizing ionic losses and improving long-term operational stability.

While continuous illumination is typically used to evaluate long-term stability at maximum power point (MPP), this approach does not capture the dynamic nature of real-world outdoor operation of PSCs. In practice, PSCs are subjected to fluctuating irradiance, including periodic reduction in light intensity due to passing clouds or diurnal cycles. These transient dark (or low

light) intervals may enable ion-mediated recovery processes. In this context, this study provides a crucial missing link between controlled laboratory measurements and actual outdoor performance. The interplay between degradation under illumination and recovery during dark intervals plays an important role in sustaining long-term performance and mitigating cumulative degradation under real-world operating conditions.

Supporting Information

Supplemental information can be found online at XXXXXXXXX. Full details of experimental procedures can be found in the Supplemental Information.

Acknowledgments

F.L. acknowledges the Volkswagen Foundation for Funding via the Freigeist Program. P.F and F.L. acknowledge the DFG for funding via the SPP2196 (HIPSTER:PRO and SURPRISEII). J.T. acknowledges funding from the Alexander von Humboldt foundation through the Humboldt Research Fellowship program. M.S. acknowledges funding support from The Chinese University of Hong Kong (CUHK) through the Vice-Chancellor Early Career Professorship Scheme, the Research Grants Council (RGC) under the NSCF/RGC Joint Research Scheme (N_CUHK414/24) and the Young Collaborative Research Fund (C4069-25YF), and the Innovation and Technology Commission (ITC) via the ITF Seed Fund (ITS/239/23).

Competing Interests

M.S. and F.L. are co-founders of SolarSense Technologies Ltd.

Author Contributions

P.F. conceived the idea, fabricated samples, designed and conducted the experiments, and prepared the manuscript under the supervision of F.L.. P.F., B.S., prepared samples for investigation. F.P. helped with sample preparation. A.F. conducted GIXRD and time-resolved

PL. T.H. and J.H. helped with the in-situ XRD setup. F.L., M.S., J.T, A.F., and S.S. helped with the interpretation and analysis of the results during the project. All the authors discussed the results and commented on the manuscript.

References

1. Finkenauer, B. P., Akriti, Ma, K. & Dou, L. Degradation and Self-Healing in Perovskite Solar Cells. *ACS Applied Materials and Interfaces* vol. 14 24073–24088 Preprint at https://doi.org/10.1021/acsami.2c01925 (2022).

2. Thiesbrummel, J. *et al.* Ion-induced field screening as a dominant factor in perovskite solar cell operational stability. *Nat. Energy* **9**, 664–676 (2024).

3. Delugas, P., Caddeo, C., Filippetti, A. & Mattoni, A. Thermally Activated Point Defect Diffusion in Methylammonium Lead Trihalide: Anisotropic and Ultrahigh Mobility of Iodine. *Journal of Physical Chemistry Letters* **7**, 2356–2361 (2016).

4. El-Mellouhi, F. *et al.* Hydrogen Bonding and Stability of Hybrid Organic–Inorganic Perovskites. *ChemSusChem* **9**, 2648–2655 (2016).

5. Motta, C. *et al.* Revealing the role of organic cations in hybrid halide perovskite CH3 NH3PbI3. *Nat. Commun.* **6**, (2015).

6. Amat, A. *et al.* Cation-induced band-gap tuning in organohalide perovskites: Interplay of spin-orbit coupling and octahedra tilting. *Nano Lett.* **14**, 3608–3616 (2014).

7. Lang, F. *et al.* Radiation Hardness and Self-Healing of Perovskite Solar Cells. *Advanced Materials* **28**, 8726–8731 (2016).

8. Bag, M. *et al.* Kinetics of Ion Transport in Perovskite Active Layers and Its Implications for Active Layer Stability. *J. Am. Chem. Soc.* **137**, 13130–13137 (2015).

9. Tress, W. Metal Halide Perovskites as Mixed Electronic-Ionic Conductors: Challenges and Opportunities - From Hysteresis to Memristivity. *Journal of Physical Chemistry Letters* vol. 8 3106–3114 Preprint at https://doi.org/10.1021/acs.jpclett.7b00975 (2017).

10. Mizusaki, J., Arai, K. & Fueki, K. *IONIC CONDUCTION OF THE PEROVSKITE-TYPE HALIDES*. *Solid State Ionics* vol. 11 (1983).

11. Schwenzer, J. A. *et al.* Temperature Variation-Induced Performance Decline of Perovskite Solar Cells. *ACS Appl. Mater. Interfaces* **10**, 16390–16399 (2018).

12. Zai, H., Ma, Y., Chen, Q. & Zhou, H. Ion migration in halide perovskite solar cells: Mechanism, characterization, impact and suppression. *Journal of Energy Chemistry* **63**, 528–549 (2021).

13. Domanski, K. *et al.* Migration of cations induces reversible performance losses over day/night cycling in perovskite solar cells. *Energy Environ. Sci.* **10**, 604–613 (2017).

14. Senocrate, A. & Maier, J. Solid-State Ionics of Hybrid Halide Perovskites. *J. Am. Chem. Soc.* **141**, 8382–8396 (2019).

15. Walsh, A. & Stranks, S. D. Taking Control of Ion Transport in Halide Perovskite Solar Cells. *ACS Energy Lett.* **3**, 1983–1990 (2018).

16. Eames, C. *et al.* Ionic transport in hybrid lead iodide perovskite solar cells. *Nat. Commun.* **6**, (2015).

17. Le Corre, V. M. *et al.* Quantification of Efficiency Losses Due to Mobile Ions in Perovskite Solar Cells via Fast Hysteresis Measurements. *Solar RRL* **6**, (2022).

18. Tress, W. *et al.* Understanding the rate-dependent J-V hysteresis, slow time component, and aging in CH3NH3PbI3 perovskite solar cells: The role of a compensated electric field. *Energy Environ. Sci.* **8**, 995–1004 (2015).

19. Thiesbrummel, J. *et al.* Universal Current Losses in Perovskite Solar Cells Due to Mobile Ions. *Adv. Energy Mater.* **11**, (2021).

20. Zheng, X. *et al.* Correlations of Ionic Migration and Deep-Level Traps Leads to Surface Defect Formation in Perovskite Solar Cells. *Journal of Physical Chemistry C* **125**, 19551–19559 (2021).

21. Warby, J. *et al.* Mismatch of Quasi–Fermi Level Splitting and Voc in Perovskite Solar Cells. *Adv. Energy Mater.* **13**, (2023).

22. Almora, O., Miravet, D., Gelmetti, I. & Garcia-Belmonte, G. Long-Term Field Screening by Mobile Ions in Thick Metal Halide Perovskites: Understanding Saturation Currents. *Physica Status Solidi - Rapid Research Letters* **16**, (2022).

23. Zhao, Y. *et al.* Mobile-Ion-Induced Degradation of Organic Hole-Selective Layers in Perovskite Solar Cells. *Journal of Physical Chemistry C* **121**, 14517–14523 (2017).

24. Kalasariya, N. *et al.* How Halide Segregation Governs the Ion Density Evolution and Ionic Performance Losses: From Degradation to Recovery. *Adv. Energy Mater.* https://doi.org/10.1002/aenm.202503866 (2026) doi:10.1002/aenm.202503866.

25. Lee, H., Ko, D. & Lee, C. Direct Evidence of Ion-Migration-Induced Degradation of Ultrabright Perovskite Light-Emitting Diodes. *ACS Appl. Mater. Interfaces* **11**, 11667–11673 (2019).

26. Besleaga, C. *et al.* Iodine Migration and Degradation of Perovskite Solar Cells Enhanced by Metallic Electrodes. *Journal of Physical Chemistry Letters* **7**, 5168–5175 (2016).

27. Guerrero, A. *et al.* Interfacial degradation of planar lead halide perovskite solar cells. *ACS Nano* **10**, 218–224 (2016).

28. Domanski, K. *et al.* Migration of cations induces reversible performance losses over day/night cycling in perovskite solar cells. *Energy Environ. Sci.* **10**, 604–613 (2017).

29. Gillespie, S. C. *et al.* Excitation Intervals Enhance Performance in Perovskite Solar Cells. *ACS Appl. Mater. Interfaces* **17**, 59476–59485 (2025).

30. Thiesbrummel, J. *et al.* Ion migration in perovskite solar cells. *Nature Reviews Chemistry* Preprint at https://doi.org/10.1038/s41570-025-00790-8 (2026).

31. Domanski, K. *et al.* Migration of cations induces reversible performance losses over day/night cycling in perovskite solar cells. *Energy Environ. Sci.* **10**, 604–613 (2017).

32. Jiang, L. *et al.* Fatigue stability of CH 3 NH 3 PbI 3 based perovskite solar cells in day/night cycling. *Nano Energy* **58**, 687–694 (2019).

33. Khenkin, M. *et al.* Light cycling as a key to understanding the outdoor behaviour of perovskite solar cells. *Energy Environ. Sci.* **17**, 602–610 (2023).

34. Khenkin, M. V. *et al.* Dynamics of Photoinduced Degradation of Perovskite Photovoltaics: From Reversible to Irreversible Processes. *ACS Appl. Energy Mater.* **1**, 799–806 (2018).

35. Remec, M. *et al.* Seasonality in Perovskite Solar Cells: Insights from 4 Years of Outdoor Data. *Adv. Energy Mater.* **15**, (2025).

36. Gupta, R. K. *et al.* Seasonal Effects on Outdoor Stability of Perovskite Solar Cells. *Adv. Energy Mater.* **15**, (2025).

37. Seid, B. A. *et al.* Mitigating Mobile-Ion-Induced Instabilities and Performance Losses in 2D Passivated Perovskite Solar Cells. *Advanced Materials* **37**, (2025).

38. Penã-Camargo, F. *et al.* Halide Segregation versus Interfacial Recombination in Bromide-Rich Wide-Gap Perovskite Solar Cells. *ACS Energy Lett.* **5**, 2728–2736 (2020).

39. Hoke, E. T. *et al.* Reversible photo-induced trap formation in mixed-halide hybrid perovskites for photovoltaics. *Chem. Sci.* **6**, 613–617 (2015).

40. Barker, A. J. *et al.* Defect-Assisted Photoinduced Halide Segregation in Mixed-Halide Perovskite Thin Films. *ACS Energy Lett.* **2**, 1416–1424 (2017).

41. Le Corre, V. M. *et al.* Quantification of Efficiency Losses Due to Mobile Ions in Perovskite Solar Cells via Fast Hysteresis Measurements. *Solar RRL* **6**, (2022).

42. Sowmeeh, P. F. *et al.* Minimizing Ionic Losses in DMSO-Free Tin-Based Perovskite Solar Cells. *ACS Energy Lett.* **10**, 6215–6222 (2025).

43. H. Balaguera, E. *et al.* 'Ion-freeze' efficiency in perovskite solar cells: time scales for ion immobilization. *EES Solar* **1**, 1051–1060 (2025).

44. Thiesbrummel, J. *et al.* Ion-induced field screening as a dominant factor in perovskite solar cell operational stability. *Nat. Energy* **9**, 664–676 (2024).

45. Rostamzadeh, H. & Montazeri, H. On the role of thermo-electro-ionic dynamics in hysteresis and transient performance of perovskite solar cells. *Energy Environ. Sci.* https://doi.org/10.1039/d5ee05840f (2026) doi:10.1039/d5ee05840f.

46. Kumar, M. *et al.* Effect of Thermal Stress on the Ion Density and Mobility Distribution in Perovskite Solar Cells. *Journal of Physical Chemistry Letters* **17**, 1527–1533 (2026).

Supplementary Files

This is a list of supplementary files associated with this preprint. Click to download.

- ReversingdegradationSIforozietal.pdf